



Short communication

Measurement of effective oxygen diffusivity in electrodes for proton exchange membrane fuel cells

Zhiqiang Yu*, Robert N. Carter

General Motors Corporation, Fuel Cell Activities, Honeoye Falls, NY 14472, USA

ARTICLE INFO

Article history:

Received 16 July 2009

Received in revised form 24 August 2009

Accepted 25 August 2009

Available online 1 September 2009

Keywords:

Proton exchange membrane fuel cell

Diffusion

Relative humidity

Porosity

Tortuosity

Electrode

ABSTRACT

This paper describes a novel method to measure directly effective diffusivity in electrodes as a function of temperature and relative humidity (RH) at conditions that are relevant for proton exchange membrane fuel cells (PEMFCs). The efficacy of this method to measure effective oxygen diffusivity ($D_{O_2}^{eff}$) is demonstrated with measurements of a series of electrodes of varying the ionomer-to-carbon weight ratio (I/C ratio). The measured $D_{O_2}^{eff}$ decreases sharply with increasing I/C ratio from 0.5 to 1.5 at the same RH, and reduces gradually with increasing RH from 0% to 100% at the same I/C ratio. The measured $D_{O_2}^{eff}$ is considerably smaller than the calculated one using the Bruggeman correction, indicating the Bruggeman correction drastically underestimates the tortuosity with increasing I/C ratio in PEMFC electrodes.

© 2009 Elsevier B.V. All rights reserved.

1. Introduction

The heart of a PEMFC is a three-layer assembly comprised of a proton-conductive membrane sandwiched between anode and cathode electrodes. Electrodes typically contain Pt nanoparticles as catalyst, carbon black as support for Pt nanoparticles, and ionomer as proton (H^+) conductor and binder. Electrodes must be sufficiently porous to transport gases and water vapor to carry out electrochemical reactions inside them. To improve the performance of PEMFCs, it is essential to identify and understand different voltage losses. The cell voltage (E_{cell}) of PEMFCs can be represented by the following equation [1]:

$$E_{cell} = E_{rev} - \eta_{HOR} - |\eta_{ORR}| - i \cdot (R_{e-} + R_{H^+,mem} + R_{H^+,An} + R_{H^+,Ca}) - \eta_{tx(gas)}, \quad (1)$$

where E_{rev} is the thermodynamic potential, η_{HOR} is the anode overpotential due to hydrogen oxidation reaction (HOR), η_{ORR} is the cathode overpotential due to oxygen reduction reaction (ORR), i is the applied current density, R_{e-} is the electronic resistance, $R_{H^+,mem}$, $R_{H^+,An}$, and $R_{H^+,Ca}$ are the proton resistances in the membrane, anode, and cathode, respectively, $\eta_{tx(gas)}$ is the gas-diffusion overpotential caused by the hydrogen and oxygen concentration gradients in the electrodes due to gas transport resistances. Except

for $\eta_{tx(gas)}$, these voltage-loss terms can be adequately determined based on various electrochemical measurements [2–5]. $\eta_{tx(gas)}$ is often split into two components: a dry component that depends on the microstructure of the porous gas-diffusion media (GDL) and electrode layers that the gas must transport through, and a wet component that is a function of the operating condition combined with the ability of the cell's components to reject liquid water. Clearly, the effective diffusivity of the electrode layer and its dependence on RH are important to fully characterize the gas transport resistance of PEMFCs.

To our knowledge, there is no reported method capable of directly measuring gas effective diffusivity of PEMFC electrodes under the conditions relevant to the PEMFC operating conditions. The Bruggeman correction which is commonly used to estimate gas effective diffusivity is reported to likely lead to overestimation for electrodes with low porosities [6,7]. While one can use traditional analysis techniques such as mercury intrusion porosimetry (MIP) and nitrogen adsorption with Barret–Joiner–Helenda (BJH) method to characterize the porosity of electrodes, these techniques are restricted to dry analysis conditions. Given that the ionomer in the electrode is highly hygroscopic and swells upon humidification, it is important to be able to characterize the electrode layer's porosity under conditions more relevant to fuel cell operation. Additionally, the thickness and loading of the electrode layer (typically 10 μm thick and 0.4 $\text{mg}_{Pt} \text{cm}^{-2}$, respectively) combine to make it difficult to use representative samples in traditional analysis techniques. The novel method described herein addresses these shortcomings by measuring the effective diffusivity in an electrode layer under

* Corresponding author. Tel.: +1 585 624 6653; fax: +1 585 624 6680.

E-mail addresses: zhiqiang.yu@gm.com, zhiqiangyu2003@hotmail.com (Z. Yu).

Nomenclature

List of parameters

C_{air}	the molar oxygen concentration in the air channel (mol cm ⁻³)
C_x	the molar oxygen concentration in the nitrogen channel (mol cm ⁻³)
$C_{x=0}$	the molar oxygen concentration in the inlet of the nitrogen channel (mol cm ⁻³)
$C_{x=L}$	the molar oxygen concentration at the exhaust of the nitrogen channel (mol cm ⁻³)
C_y	the molar oxygen concentration inside the electrode in the y direction as indicated in Fig. 3 (mol cm ⁻³)
$D_{O_2}^{eff}$	the effective oxygen diffusivity (cm ² s ⁻¹)
D_{O_2}	the oxygen free space diffusivity (cm ² s ⁻¹)
L	the length of the nitrogen channel (19 cm)
m	the diffusive length between the air and nitrogen channels (0.2 cm)
J_y	the molar diffusion flux of oxygen from both air channels to the nitrogen channel (mol cm ⁻² s ⁻¹)
Q	the gas volumetric flow rate in the nitrogen channel (cm ³ s ⁻¹)
Δx	the length of the illustrated segment in Fig. 3 (cm)
δ	the thickness of the electrode (cm)
ε	the void fraction of the electrode
τ	the tortuosity of the electrode
L_{Pt}	the Pt loading in the electrode (mg _{Pt} cm ⁻² _{electrode})
L_{carbon}	the carbon loading in the electrode (mg _{carbon} cm ⁻² _{electrode})
$L_{ionomer}$	the ionomer loading in the electrode (mg _{ionomer} cm ⁻² _{electrode})
ρ_{Pt}	Pt density (21.5 g cm ⁻³)
ρ_{carbon}	carbon density (2.2 g cm ⁻³)
$\rho_{ionomer}$	ionomer density (2.0 g cm ⁻³)

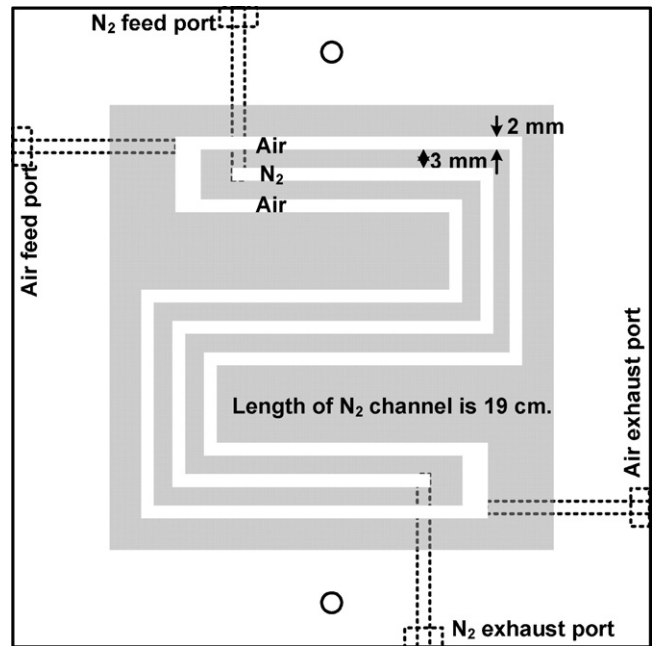


Fig. 2. Plan-view of the flow field.

the $D_{O_2}^{eff}$ measurements. The “in-plane” diffusion means that the diffusion direction is parallel to the electrode surface (the x direction in Fig. 1). In operating PEMFCs, oxygen is more likely to experience “through-plane” diffusion in electrodes, where the diffusion direction is perpendicular to the electrode plane (the y direction in Fig. 1). However, $D_{O_2}^{eff}$ in porous PEMFC electrodes should be the same no matter oxygen is in either “in-plane” or “through-plane” diffusion. Fig. 1 shows the porous electrode film coated on ethylene tetrafluoroethylene (ETFE) is tested by mounting it between a flow field with three parallel gas channels and a blank flow field. Air flows through the two outer channels and nitrogen through the center channel. This arrangement results in oxygen diffusion from the air channel into the nitrogen channel via the porous electrode. Because the nitrogen channel is flanked on both sides by the air channels, the rate of oxygen diffusion is effectively doubled, thereby reducing the required length of flow channel to achieve a measurable oxygen concentration at the exhaust of the nitrogen channel.

A gasket made of silicone rubber with the thickness of 250 μ m (Durometer 35A, McMaster-Carr) is used to seal the air and nitrogen channels under a load of 5.3 kN. The gasket is cut by laser to match the channels. The width of the gasket that seals the lands between the air and nitrogen channels are 2 mm as shown in Fig. 1, allowing some tolerance for placement of the gasket to ensure that it is completely supported by the 3 mm wide flow field lands. Placement of the gasket is important because the width of the gasket between the air and nitrogen channels defines the oxygen diffusion length used in the calculation of $D_{O_2}^{eff}$.

Fig. 2 shows the plan-view of the flow field depicting the features of the air and nitrogen channels. Air and nitrogen co-flow through the flow field with a channel length of 19 cm. The oxygen concentration at the exhaust of the nitrogen channel is monitored by a self-heated oxygen sensor (model: LZA03-E1, NGK Spark Plugs, Michigan). The test is run with the two gas streams held at ambient pressure (101.3 kPa). The pressure drops in the air and nitrogen channels are calculated to be 21 and 17 Pa, respectively. The maximum pressure gradient between the air and nitrogen channel is only 4 Pa when both air and nitrogen are flowing. Even if a pressure gradient of 10 kPa exists between the air and nitrogen channels, the resulting oxygen bulk convection is calculated to account for less

conditions similar to those of an operating PEMFC and at a sample scale of 50 cm². The efficacy of the developed method is demonstrated in measurements of oxygen effective diffusivity ($D_{O_2}^{eff}$) in electrodes with a range of ionomer-to-carbon weight ratios (I/C ratio).

2. Measurement of $D_{O_2}^{eff}$ inside electrodes

2.1. Method description

The measurement is based on oxygen “in-plane” diffusion in electrodes on a conventional PEMFC platform with 50 cm² flow fields. Fig. 1 shows the schematic cross-section of the cell fixture for

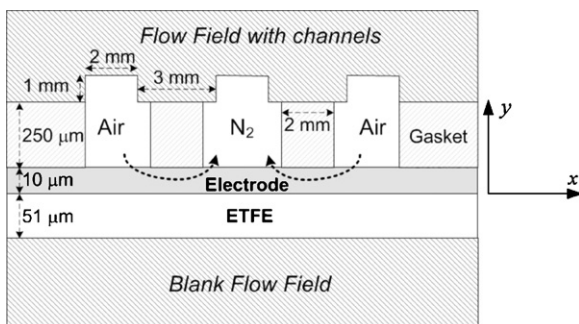


Fig. 1. Schematic cross-section of the cell fixture.

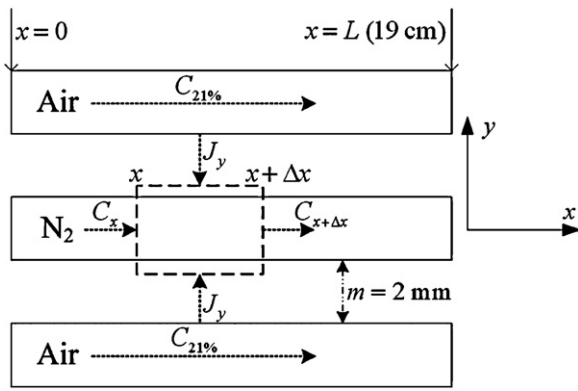


Fig. 3. Illustration of the oxygen mass balance over the nitrogen channel.

than 2.13% of the oxygen diffusion flux in the $D_{O_2}^{eff}$ measurements for electrodes with I/C ratios of 0.5 and 1.0. Thus, the driving force for forced convective flow between the adjacent air and nitrogen channels is negligible, and the transport of oxygen from the air channels to the nitrogen channel is driven only by the oxygen concentration gradient. Because of the minimal pressure gradient between the external air channel and the ambient, it is assumed that there is no much oxygen in the air channel diffusing through the electrode to the ambient. Thus, oxygen can only diffuse from the air channels to the nitrogen channel through the porous electrode.

To measure the oxygen diffusion length accurately under the load, a piece of Fuji Prescale film for super low pressure (FujiFilm, Japan) is inserted between the electrode and the gasket and then compressed by the two flow fields. Under the compression, the Fuji Prescale film develops colorful strips due to the pressure exerted by the gasket between the air and nitrogen channels. The width of colorful strips on the pressure-paper reflects that the expansion of the 2 mm wide gasket under a load of 5.3 kN is negligible. Thus, the oxygen diffusion length is 2 mm in the calculation of $D_{O_2}^{eff}$.

2.2. Calculation of $D_{O_2}^{eff}$

As described above, oxygen is designed to “in-plane” diffuse through a 2 mm wide porous electrode due to the oxygen concentration gradient between the air channels and the nitrogen channel. Since the electrode thickness ($10 \mu\text{m}$) is 200 times smaller than the oxygen diffusion length (2 mm), the oxygen concentration inside the electrode is assumed to be the same in the y direction in Fig. 1. In addition, the oxygen concentration inside the electrode which is under the air or nitrogen channel is assumed to be the same in the x direction in Fig. 1. Therefore, the oxygen transport in this study is simplified to an issue of oxygen diffusion due to the concentration gradient through a porous electrode which is 2 mm wide, $10 \mu\text{m}$ thick, and 19 cm long.

Fig. 3 illustrates an oxygen mass balance over a segment of the nitrogen channel for developing the equation in the calculation of $D_{O_2}^{eff}$. It is expressed as follows:

$$Q \times (C_{x+\Delta x} - C_x) + 2J_y \times \Delta x \times \delta = 0 \quad (2)$$

where Q is the gas volumetric flow rate, C_x is the molar oxygen concentration in the nitrogen channel, J_y is the molar diffusion flux of oxygen from both air channels to the nitrogen channel, Δx is the length of the illustrated segment in Fig. 3, and δ is the thickness of the electrode. In the limit of $\Delta x \rightarrow 0$, Eq. (2) becomes:

$$\frac{dC_x}{dx} = -\frac{2J_y\delta}{Q} \quad (3)$$

Because the air and nitrogen channels are kept at the same temperature, pressure, and RH, and oxygen bulk convection between the air channels and the nitrogen channel is negligible as discussed above, oxygen transport from the air channels to the nitrogen is assumed to be an oxygen-nitrogen binary diffusion. Thus J_y can be expressed according to Fick's law of diffusion as follows:

$$J_y = -D_{O_2}^{eff} \frac{dC_y}{dy} \quad (4)$$

where $D_{O_2}^{eff}$ is the effective oxygen diffusivity, C_y is the molar oxygen concentration inside the electrode in the y direction in Fig. 3. In the present study, the test conditions and fixture design are chosen such that the measurement of PEMFC electrodes would result in oxygen concentrations of less than 400 ppm in the nitrogen channel, which is 500 times lower than 21% oxygen in the air channels. Thus, the oxygen concentration in the air channel (C_{air}) is considered to be constant at 21% although a trace amount of oxygen diffuses from the air channels to the nitrogen channel. Consequently, J_y can be assumed to be constant down the length of the channels because the oxygen concentration gradient (i.e., 21% vs. at most 400 ppm) between the air channels and the nitrogen channel is basically unchanged. Thus, J_y in Eq. (4) can be simplified as follows:

$$J_y = -D_{O_2}^{eff} \frac{C_{air}}{m} \quad (5)$$

where C_{air} is the molar oxygen concentration in the air channel (defined by the operating temperature and RH) and m is the diffusive length scale defined by the sealing gasket width (2 mm).

Thus, with a constant J_y and a boundary condition as $C_{x=0} = 0$, the oxygen concentration at the exhaust of the nitrogen channel ($C_{x=L}$) can be derived from Eq. (3) as follows:

$$C_{x=L} = -\frac{2J_y\delta L}{Q} \quad (6)$$

Then, combination of Eqs. (5) and (6) yields the following expression for calculating $D_{O_2}^{eff}$:

$$D_{O_2}^{eff} = \frac{C_{x=L} Q m}{2\delta L C_{air}} \quad (7)$$

Note that $C_{x=L}$, C_{air} , and Q are all RH-dependant variables in the calculation.

3. Experimental details

Carbon-supported Pt catalyst (50 wt.% Pt/carbon; Tanaka, Japan) and ionomer solutions (5 wt.% Nafion® in organic solvents, 900 equivalent weight (EW); DuPont, USA) were ballmilled in a mixture of water and ethanol for 72 h. The resulting catalyst inks were then coated by Meyer rod coating on blank ethylene tetrafluoroethylene (ETFE) films at a catalyst loading of $0.4 \text{ mg}_{Pt} \text{ cm}^{-2}$ (note: cm^2 refers to the geometric area of electrodes). Electrodes with I/C ratios of 0.5, 1.0, and 1.5 were fabricated and then die-cut into 50 cm^2 samples.

The electrodes are mounted in the cell fixture shown in Fig. 1 and then compressed at a load of 5.3 kN, giving 1.41 MPa pressure on the porous electrode film. The cell fixture is heated to 80°C . Air and nitrogen flow rates into the saturators are 300 and 150 sccm, respectively. Air and nitrogen are vented to ambient after the flow field. The connection between saturators and the flow field as well as between the flow field and the oxygen sensor are heated to prevent water condensation in those regions. This is critical for maintaining the desired RH in the air and nitrogen channels as well as preventing artifacts in the apparent oxygen diffusion due to the presence of liquid water in the cell fixture. The temperature of the

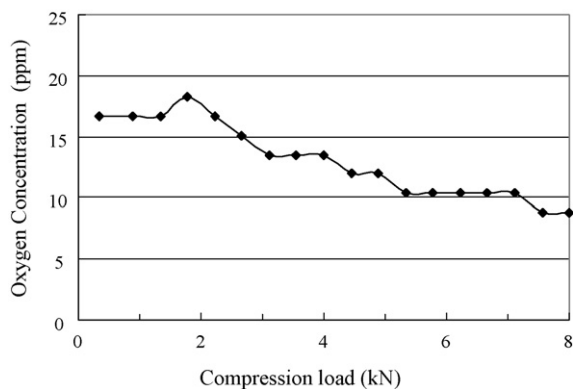


Fig. 4. Results of the control test showing the oxygen concentration in the exhaust of the nitrogen channel as a function of compressive load applied to the cell fixture. The test sample is a piece of uncoated ETFE. Test conditions are 80 °C, 300/150 sccm for air/nitrogen, 101 kPa, and 0% RH.

saturators is adjusted to control the RH in air and nitrogen channels to values of 20%, 40%, 60%, 80%, 90%, and 100%. Additionally, the gas streams can be bypassed around their respective saturators to obtain 0% RH. Ten cycles of RH sweep from 20% to 100% are conducted over each electrode to get stable measurements. Following the ten cycles of RH sweep, the measurement at 0% RH is carried out for 5 h to get stable value. The oxygen concentration in the exhaust of the nitrogen channel is recorded every 10 s. At each condition, the oxygen concentration is averaged over stable data in a period of 30 min. Three repeats with new samples are conducted to determine the repeatability of this method. Scanning electron microscopy (SEM, FEI Quanta 400) is used to measure the thickness of electrodes before and after the tests. The fresh electrodes on ETFE are embedded in a standard epoxy resin (Epoxy, Struers) for the cross-section SEM image, while the tested electrodes transferred onto silicone gasket are self-supported for the same analysis.

4. Results and discussion

A gasket is used to seal the air and nitrogen channels. A control test was performed to determine what compressive load is necessary to achieve adequate sealing without inducing excessive stress on the porous electrode structure and potentially causing deformation. In the control measurement, an ETFE film without the electrode coating is mounted in the cell fixture to test the extent of sealing with increasing compression load at 80 °C, 101 kPa and 0% RH. Fig. 4 shows the results of this test, where the oxygen concentration in the exhaust of the nitrogen channel is plotted as a function of the compression load. The oxygen concentration decreases from about 18 to 10 ppm as the compression load increases up to 5.3 kN, where upon it remains fairly steady up to 8.0 kN. Considering the oxygen diffusivity in silicone rubber is typically in the order of 10^{-7} to 10^{-6} $\text{cm}^2 \text{s}^{-1}$ [8], permeation of oxygen through the silicone gasket should result in an oxygen concentration of less than 0.2 ppm in the nitrogen channel. This analysis indicates that the background oxygen concentration of 10 ppm is mostly due to small leaks at the gasket seal. The oxygen concentration in the nitrogen exhaust in the tests for typical electrodes (i.e., I/C ratio from 0.5 to 1.0) ranges generally from 120 to 350 ppm, which is many times larger than the 10 ppm baseline. Thus, a compression load of 5.3 kN on flow fields is chosen in this method to achieve adequate sealing for the air and nitrogen channels. The oxygen concentration of 10 ppm is assumed as a baseline and subtracted from the oxygen concentrations measured in the electrode tests.

Fig. 5 presents the last two cycles of oxygen concentrations at the exhaust of the nitrogen channel ($C_{x=L}$ in ppm) at varying RH values

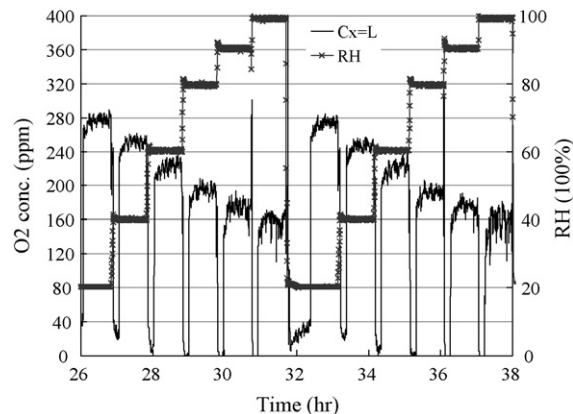


Fig. 5. The last two cycles of oxygen concentrations at the exhaust of the nitrogen channel ($C_{x=L}$) with RH sweep from 20% to 100% over an electrode with I/C of 0.5. Ten cycles of RH sweep are conducted over each electrode to get stable oxygen concentrations.

over an electrode with I/C ratio of 0.5. This result demonstrates that $C_{x=L}$ is a steady-state value at each RH condition and drastically sensitive to the RH change over the electrode. Note that $C_{x=L}$ needs to be converted into the unit of molar concentration for calculating $D_{\text{O}_2}^{\text{eff}}$ in Eq. (7), thereby incorporating the dilution effect of increasing RH into the calculation.

Fig. 6 displays SEM images of the cross-section of electrodes with an I/C of 1.0 before and after the $D_{\text{O}_2}^{\text{eff}}$ measurement. The fractures observed in the tested electrode are caused by sample preparation for SEM analysis. The SEM images indicate no change in the electrode thickness, thereby showing the porous electrode does not collapse under the 5.3 kN compression load. More SEM analysis (not presented) shows that electrodes with I/C ratios of 0.5 and 1.5 also have the same thickness of 10 μm after the $D_{\text{O}_2}^{\text{eff}}$ measurements. Thus, a thickness of 10 μm is used in Eq. (7) to calculate $D_{\text{O}_2}^{\text{eff}}$ for all the three types of electrodes.

Fig. 7 displays the measured $D_{\text{O}_2}^{\text{eff}}$ for electrodes with I/C ratios of 0.5, 1.0, and 1.5 as a function of RH. The results show that the measured $D_{\text{O}_2}^{\text{eff}}$ of electrodes decreases sharply with increasing I/C ratio at the same RH but reduces gradually with increasing RH at the same I/C ratio. For example, at 0% RH, the measured $D_{\text{O}_2}^{\text{eff}}$ decreases 70% and 95% as I/C ratios increases from 0.5 to 1.0 and 1.5, respectively. In contrast, the measured $D_{\text{O}_2}^{\text{eff}}$ of the electrodes with I/C ratios of 0.5 and 1.0 correspondingly decrease 20% and 25% as RH increases from 0% to 100%. Given that the electrode thickness is observed in SEM analysis to be independent of the I/C ratio, increasing the I/C ratio from 0.5 to 1.5 triples the ionomer volume fraction and correspondingly reduces the electrode void fraction. Due to the ionomer's nature of swelling upon hydration, one expects to see a decrease in the diffusivity as RH is increased. The measured $D_{\text{O}_2}^{\text{eff}}$ of the electrode with I/C ratio of 1.5 is significantly smaller than those of electrodes with I/C ratios of 0.5 and 1.0, indicating the severe ionomer filling and blocking of pores inside the electrode with I/C ratio of 1.5 for oxygen diffusion. Furthermore, the measured $D_{\text{O}_2}^{\text{eff}}$ of the electrode with I/C ratio of 1.5 appears independent on RH because (i) its absolute value is too small to show the dependence and (ii) the developed method may lose its sensitivity when measuring the value of $C_{x=L}$ in the range of 15–32 ppm with a 10 ppm baseline for the oxygen concentration.

Fig. 7 also presents the remarkable reproducibility among the three replicate tests for each type of electrodes, further demonstrating the efficacy of the developed method for measuring $D_{\text{O}_2}^{\text{eff}}$

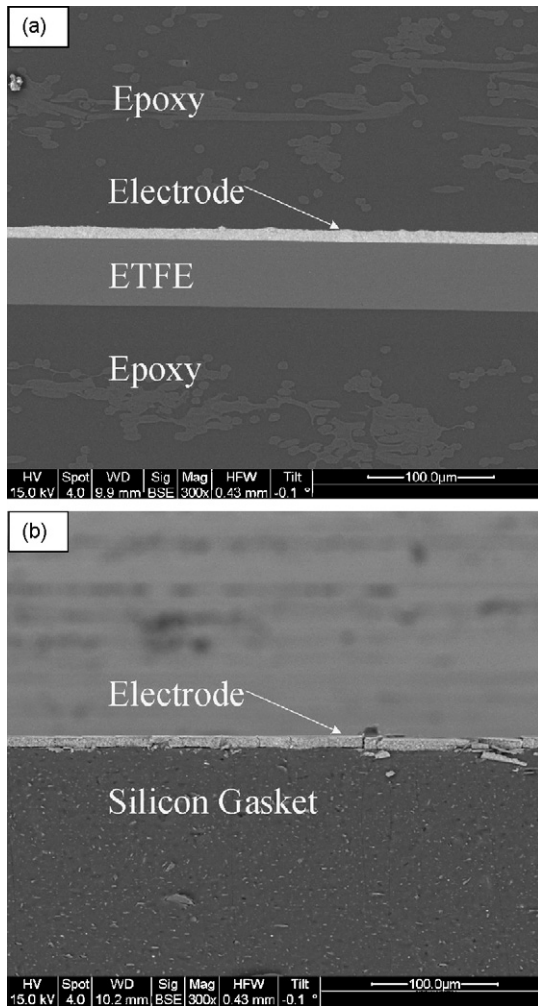


Fig. 6. SEM images of the cross-section of (a) a fresh electrode with I/C of 1.0 coated on ETFE and (b) a tested electrode with I/C of 1.0 supported on the silicone rubber gasket. Note that the tested electrode film always transfers to the silicone gasket after being compressed in the cell fixture.

in PEMFC electrodes. Stumper reported that $D_{O_2}^{eff}$ in combination of the gas-diffusion layer and the catalyst layer was measured to be between 0.0061 and 0.0072 $\text{cm}^2 \text{s}^{-1}$ [9]. Although he did not report the catalyst loading or I/C ratio in the catalyst layer, his measurements are reasonably close to the results repeated here for an electrode with I/C ratio of 1.0.

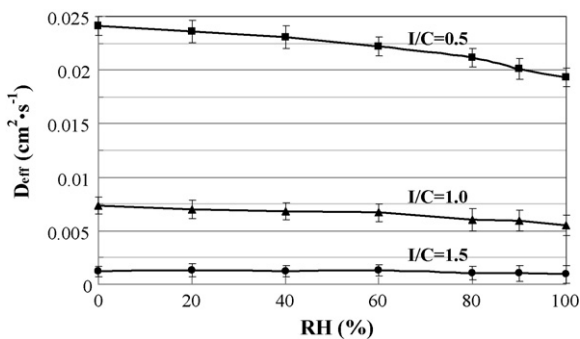


Fig. 7. Measured $D_{O_2}^{eff}$ (average of three replicates) as a function of RH for electrodes with I/C ratios of 0.5, 1.0, and 1.5. Test conditions are 80 °C, 300/150 sccm for air/nitrogen, and 101 kPa. The error bars indicate 95% confidence limits.

Table 1

Summary of measured $D_{O_2}^{eff}$, calculated porosities, and calculated $D_{O_2}^{eff}$ ^a.

Electrodes	Measured $D_{O_2}^{eff}$ ^b	Calculated porosity	Calculated $D_{O_2}^{eff}$
I/C 0.5	0.02410	68.1%	0.155
I/C 1.0	0.00734	58.1%	0.122
I/C 1.5	0.00119	48.1%	0.092

^a Conditions: 80 °C, 101 kPa, and 0% RH.

^b Unit: $\text{cm}^2 \text{s}^{-1}$.

According to its definition, $D_{O_2}^{eff}$ is expressed as follows:

$$D_{O_2}^{eff} = \frac{\varepsilon}{\tau} D_{O_2}, \quad (8)$$

where ε is the void fraction, τ is the tortuosity, and D_{O_2} is the oxygen free space diffusivity. Typically, the Bruggeman expression is used to estimate the tortuosity as [7]:

$$\tau = \varepsilon^{-0.5}. \quad (9)$$

Combination of Eqs. (8) and (9) give the Bruggeman correction for $D_{O_2}^{eff}$ in PEMFC electrodes:

$$D_{O_2}^{eff} = \varepsilon^{1.5} D_{O_2}. \quad (10)$$

In the O_2 - N_2 - H_2O ternary system in PEMFC electrodes, D_{O_2} is usually estimated by the Wilke equation [10–12], with the assumption of zero flux of nitrogen and water vapor in the system:

$$D_{O_2} = \frac{1 - x_{O_2}}{(x_{N_2}/D_{O_2-N_2}) + (x_{H_2O}/D_{O_2-H_2O})}, \quad (11)$$

where x_{O_2} , x_{N_2} , and x_{H_2O} are the mole fractions of oxygen, nitrogen, and water vapor in electrodes, respectively. The binary diffusivity of oxygen and nitrogen, $D_{O_2-N_2}$, is calculated using Chapman–Enskog equation [10] and the binary diffusivity of oxygen and water vapor, $D_{O_2-H_2O}$, is calculated using Slattery–Bird equation [13]. At 80 °C, 101 kPa, and 0% RH, D_{O_2} is equivalent to $D_{O_2-N_2}$ and calculated to be 0.276 $\text{cm}^2 \text{s}^{-1}$.

The porosity of electrodes at 0% RH can be determined, since the electrode thickness as well as the mass loadings and densities of Pt, carbon, and ionomer are known. The expression for the calculated porosity of electrodes is

$$\varepsilon = 1 - \frac{(L_{Pt}/\rho_{Pt}) + (L_{carbon}/\rho_{carbon}) + (L_{ionomer}/\rho_{ionomer})}{V}, \quad (12)$$

where ε is the porosity of electrodes, L_{Pt} is the Pt loading (0.4 $\text{mg cm}^{-2}_{\text{electrode}}$ in this study), L_{carbon} is the carbon loading (0.4 $\text{mg cm}^{-2}_{\text{electrode}}$ for 50 wt.% Pt/carbon), and $L_{ionomer}$ is the ionomer loading, which equals to $L_{carbon} \times I/C$. ρ_{Pt} (21.5 g cm^{-3}) [14], ρ_{carbon} (2.2 g cm^{-3}) [14], and $\rho_{ionomer}$ (2 g cm^{-3}) [15] are densities of Pt, carbon, and ionomer, respectively. V is the geometric volume of electrodes (0.001 $\text{cm}^3 \text{cm}^{-2}_{\text{electrode}}$ in this study).

Table 1 summarizes the measured $D_{O_2}^{eff}$, the calculated porosity, and the calculated $D_{O_2}^{eff}$ using the Bruggeman correction for electrodes at 80 °C, 101 kPa, and 0% RH. Although the measured $D_{O_2}^{eff}$ decreases by 95% as I/C ratio increases from 0.5 to 1.5, the calculated porosities only reduces by 29%. Thus, the disproportionate decrease in the measured $D_{O_2}^{eff}$ is most likely attributable to an increase in the tortuosity in electrodes with increasing I/C ratio. In addition, the measured $D_{O_2}^{eff}$ is considerably smaller than the calculated $D_{O_2}^{eff}$ for all the three electrodes. The ratio of the measured $D_{O_2}^{eff}$ to the calculated $D_{O_2}^{eff}$ decreases as I/C ratio increases, indicating the Bruggeman correction drastically underestimates the tortuosity with increasing I/C ratio in PEMFC electrodes [7].

5. Conclusion

A method has been developed to measure directly gas effective diffusivity in electrodes as a function of temperature and RH under the conditions relevant to the PEMFC operating conditions. At 80 °C and 101 kPa, $D_{O_2}^{eff}$ in electrodes with I/C ratios of 0.5, 1.0, and 1.5 are measured on a 50 cm² flow field for PEMFCs, with RH varying from 0% to 100%. The measured $D_{O_2}^{eff}$ of electrodes decreases sharply with increasing I/C ratio at the same RH but reduces gradually with increasing RH at the same I/C ratio. The calculated porosity of electrodes reduces by 29% as I/C ratio increases from 0.5 to 1.5, but the measured $D_{O_2}^{eff}$ decreases by 95%, inferring a dramatic increase in the tortuosity with increasing I/C ratio. In addition, the measured $D_{O_2}^{eff}$ is considerably smaller than the calculated $D_{O_2}^{eff}$ using the Bruggeman correction for all the three electrodes, indicating that the Bruggeman correction drastically underestimates the tortuosity in PEMFC electrodes.

Acknowledgements

We would like to thank Michael K. Budinski and Mark Mathias for many fruitful discussions.

References

- [1] K.C. Neyerlin, W. Gu, J. Jorne, A. Clark Jr., H.A. Gasteiger, J. Electrochem. Soc. 154 (2007) B279.
- [2] H.A. Gasteiger, S.S. Kocha, B. Sompalli, F.T. Wagner, Appl. Catal. B 56 (2005) 9.
- [3] Y. Liu, M. Murphy, D. Baker, W. Gu, C. Ji, J. Jorne, H.A. Gasteiger, ECS Trans. 11 (2007) 473.
- [4] R.N. Carter, W. Gu, B. Brady, K. Subramanian, H.A. Gasteiger, MEA Degradation Mechanisms Studies by Current Distribution Measurements, in Handbook of Fuel Cells—Advancers in Electrocatalysts, Materials, in: Diagnostics and Durability, John Wiley & Sons, New York, 2009, p. 829.
- [5] S.S. Kocha, Principles of MEA Preparation, in Handbook of Fuel Cells—Fundamentals Technology and Applications, John Wiley & Sons, New York, 2003, pp. 538–565.
- [6] J.G. Pharoah, K. Karan, W. Sun, J. Power Sources 161 (2006) 214.
- [7] A. Weber, R. Darling, J. Newman, J. Electrochem. Soc. 151 (2004) A1715.
- [8] L.K. Mass, Permeability Properties of Plastics and Elastomers: A Guide to Packaging and Barrier Materials, William Andrew, Norwich, 2003, p. 500.
- [9] J. Stumper, H. Haas, A. Granados, J. Electrochem. Soc. 152 (2005) A837.
- [10] R.H. Perry, D.W. Green, Perry's Chemical Engineers' Handbook, McGraw-Hill, New York, 1997.
- [11] V. Gurau, F. Barbir, H. Liu, J. Electrochem. Soc. 147 (2000) 2468–2477.
- [12] P.K. Das, X. Li, Z.-S. Liu, J. Electroanal. Chem. 604 (2007) 72–90.
- [13] R.B. Bird, W.E. Stewart, E.N. Lightfoot, Transport Phenomena, Wiley, New York, 2006.
- [14] P.J. Ferreira, G.J.O. La, Y. Shao-Horn, D. Morgan, R. Makharia, S. Kocha, H.A. Gasteiger, J. Electrochem. Soc. 152 (2005).
- [15] Y. Liu, M.W. Murphy, D.R. Baker, W. Gu, C. Ji, J. Jorne, H.A. Gasteiger, J. Electrochem. Soc. 156 (2009) B970–B980.